

## Atomistic study on twinning of $\text{Cu}_2\text{O}$ quantum dots

Luying Li, Jianbo Wang, Renhui Wang, Huijun Liu, Chunlin Jia, Lili Ma, and Ying Yu

Citation: *Appl. Phys. Lett.* **89**, 113109 (2006);

View online: <https://doi.org/10.1063/1.2353807>

View Table of Contents: <http://aip.scitation.org/toc/apl/89/11>

Published by the [American Institute of Physics](#)

---

### Articles you may be interested in

Formation of  $\text{Cu}_2\text{O}$  quantum dots on  $\text{SrTiO}_3$  (100): Self-assembly and directed self-assembly

*Journal of Applied Physics* **100**, 094315 (2006); 10.1063/1.2364038

---



# Scilight

Sharp, quick summaries **illuminating**  
the latest physics research

Sign up for **FREE!**

**AIP**  
Publishing

# Atomistic study on twinning of Cu<sub>2</sub>O quantum dots

Luying Li,<sup>a)</sup> Jianbo Wang,<sup>a,b)</sup> Renhui Wang,<sup>a)</sup> and Huijun Liu

*Department of Physics, Wuhan University, Wuhan 430072, China and Key Laboratory of Acoustic and Photonic Materials and Devices of Ministry of Education, Wuhan University, Wuhan 430072, China*

Chunlin Jia

*Institut für Festkörperforschung, Forschungszentrum Jülich, 52425 Jülich, Germany*

Lili Ma and Ying Yu

*College of Physical Science and Technology, Central China Normal University, Wuhan 430079, China*

(Received 4 April 2006; accepted 17 July 2006; published online 12 September 2006)

Cu<sub>2</sub>O nanoparticles are investigated at atomic scale by high-resolution transmission electron microscopy. It is found that growth {111} twinning is the most common type of defects in these nanoparticles. The atomic structure of the twinning boundaries is determined referring to the detailed image simulations based on the structure model refined by first-principles calculation. The twin boundary plane is along a {111} oxygen plane and the twinning shows a crystallographic relation with a symmetry operation of 180° rotation around a  $\langle 111 \rangle$  axis perpendicular to the plane. The effect of the twinning on the stability of the particles is discussed. © 2006 American Institute of Physics. [DOI: 10.1063/1.2353807]

Cu<sub>2</sub>O attracts great interests of research due to its rich excitonic structure and high absorption coefficient. For far-ranging applications in photovoltaic devices and solar energy conversion process, different material forms of Cu<sub>2</sub>O such as films<sup>1</sup> and quantum dots in solutions<sup>2</sup> as well as on different substrates<sup>3,4</sup> have been prepared and studied. It is reported that the cubic phase of Cu<sub>2</sub>O is more stable than the monoclinic CuO for the crystal size below 25 nm in contrast to the case of the bulk states.<sup>5</sup> A question arises on the structure factors responsible for the stability of the cubic phase of Cu<sub>2</sub>O. In addition to the surface structure, the defect configuration in the nanoparticles may play a role in stabilization of the cubic phase. Up to now, seldom information is revealed about defects in Cu<sub>2</sub>O. Moss *et al.* reported (110) faults in Cu<sub>2</sub>O of mineralogical form in 1988.<sup>6</sup> Recently, Yin *et al.* synthesized Cu<sub>2</sub>O nanoparticles in solution and observed twinning structure by high-resolution transmission electron microscopy (HRTEM).<sup>2</sup> However, details about atomic arrangement at twin boundaries and their possible effect on the stability of nanoparticles are still in question.

Twinning concerns two or more parts of crystals which are associated with each other by certain symmetry operations. Considering the formation mechanism, twinning can be classified into two categories: deformation twinning and growth twinning. The deformation twinning has been intensively studied in both bulky materials<sup>7,8</sup> and nanocrystals.<sup>9,10</sup> In contrast the growth twinning is less understood. Recent interests in growth twinning<sup>11–14</sup> were renewed coming from the growth of nanomaterials. The twinning can be characterized by several methods. Selected area electron diffraction (SAED) analysis is the most commonly utilized technique.<sup>7,8</sup> The others include reflection high energy electron diffraction,<sup>15</sup> electron backscatter diffraction,<sup>16</sup> and HRTEM.<sup>9–13</sup> Among all those techniques, HRTEM is one

of the most powerful tools in obtaining local atomic arrangement.

In the present letter, the twin structure in Cu<sub>2</sub>O nanoparticles is investigated by means of HRTEM. Image simulation and first-principles calculation are carried out in determination of the atomic structure of the twinning boundary. The mechanism of twinning is also discussed.

The Cu<sub>2</sub>O nanoparticles are prepared on the multiwall carbon nanotubes (MWCNTs) which are synthesized by chemical vapor deposition method. In order to get oxygenated functionalities on the surface, the MWCNTs are boiled in concentrated nitric acid. The treated MWCNTs are sonicated in ethanol, together with the precursor Cu(CH<sub>3</sub>COO)<sub>2</sub>·H<sub>2</sub>O. The obtained mixture is then reacted with glycerol in a sealed reactor under N<sub>2</sub> flush. Finally, the obtained composites are washed with ethanol and dried in vacuum oven. Detailed process is presented in Ref. 4. Some as-prepared composites are sonicated in ethanol and dropped onto the holey carbon-coated multigrid, which are then dried for TEM observation.

TEM observation (mainly includes bright field image and SAED) and HRTEM characterization are performed using JEOL JEM 2010FEF electron microscope, operated at 200 kV.

Figure 1(a) shows representatively a bright field image

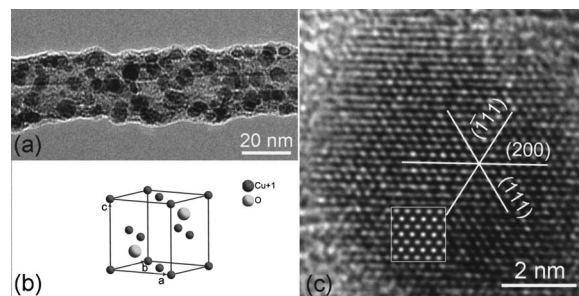


FIG. 1. (a) TEM image of a typical MWCNT coated by Cu<sub>2</sub>O quantum dots. (b) Crystal structure of Cu<sub>2</sub>O. (c) HRTEM image of a typical Cu<sub>2</sub>O particle of perfect structure.

<sup>a)</sup>Also at Center for Electron Microscopy, Wuhan University, Wuhan 430072, China.

<sup>b)</sup>Author to whom correspondence should be addressed; electronic mail: wang@whu.edu.cn

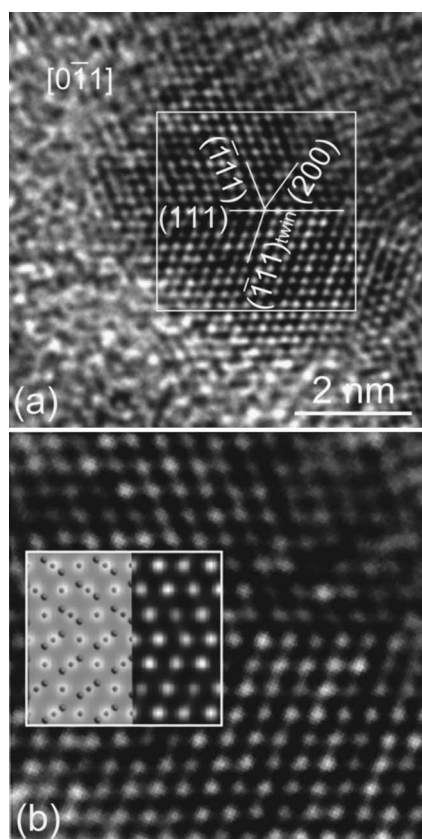


FIG. 2. (a) Representative twinning structure of  $\{111\}\langle 112 \rangle$  type with the twinning plane indexed. (b) A zoomed-in image of the part surrounded by the white frame in (a).

of  $\text{Cu}_2\text{O}$  nanoparticles on a MWCNT. It is apparently shown that the  $\text{Cu}_2\text{O}$  quantum dots distribute homogeneously on the MWCNT surface. The mean value of the particle size is obtained as 5.3 nm with narrow size distribution from statistical analysis of 766 particles. The majority of the particles are found to adopt the morphology of spherical shape. Figure 1(c) shows a  $\text{Cu}_2\text{O}$  particle which is free of defects. The simulated image [the inset in Fig. 1(c)] based on the cubic unit-cell model in Fig. 1(b) fits well to the experimental image, demonstrating that the particle has the cubic  $\text{Cu}_2\text{O}$  structure. Elemental mapping and electron energy loss near edge structure confirm the composition of  $\text{Cu}_2\text{O}$  as well. The morphology of these nanoparticles can be attributed to the high symmetry of their cubic structure as shown in Fig. 1(b). Since the role of the surface energy in determination of the total energy increases as the size of the particles decreases, the lower surface energy and smaller surface area favor the stability of the nanoparticles.<sup>5</sup> With equal volume, the sphere has the smallest surface area. The high symmetry of the cubic structure leads to less anisotropy in the surface, resulting in lower energy. These may be responsible for morphology and the structure adopted by the  $\text{Cu}_2\text{O}$  nanoparticles.

It is found that about 30% of the observed  $\text{Cu}_2\text{O}$  nanoparticles contain twinning. The twinning occurs along the  $\{111\}$  plane. Figure 2(a) shows a particle containing twinning. It is projected along the  $[0\bar{1}1]$  axis and is characterized as  $\{111\}\langle 112 \rangle$  type. The twinning boundaries are clearly shown in Fig. 2(b) in zoomed-in form.

In order to fully understand the arrangement of atoms at the twinning boundaries, structural modeling is carried out. In constructing twinning models, the normally applied opera-

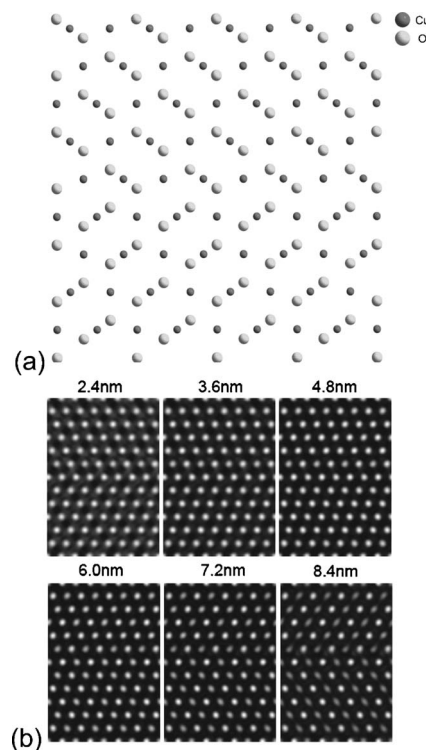


FIG. 3. (a)  $180^\circ$  rotation twinning model of  $\{111\}\langle 112 \rangle$  type before relaxation. (b) Series of simulated HRTEM images with the changed sample thickness based on the model.

tions are as follows:  $180^\circ$  rotation of one part around a crystallographic axis perpendicular to a  $\{111\}$  plane and mirror reflection of one part on a  $\{111\}$  plane. In addition, translations on the twinning plane are also considered. In the case of oxides, the stoichiometry in the boundary area must be taken into account for the charge balance. Due to the coexistence of both Cu and O sublattices, the twinning operations should avoid too small interatomic distances, in particular, the distance between the same type of ions, and nonstoichiometry.

Figure 3(a) shows a structure model of twinning obtained by  $180^\circ$  rotation around the  $[111]$  axis. The boundary plane is chosen as the  $(111)$  oxygen plane. In this model, the stoichiometry of the bulk is maintained. Across the twin boundary no too short interatomic distances appear, and the Cu–O bonding is not severely broken down. These features favor to lower the boundary energy.

HRTEM simulation is carried out based on the model shown in Fig. 3(a) employing MSSC and MACTEMPAS software packages. The left part in the white frame of Fig. 2(b) is the  $180^\circ$  rotation twin model superimposed on simulated HRTEM image. The Cu atoms in the model correspond to the bright dots in the simulated image. The right part is the simulated image based on the model for a defocus of  $-50$  nm and a sample thickness of 4 nm. The thickness is chosen according to the diameter of the  $\text{Cu}_2\text{O}$  particles. It is clear that the simulated image fits at a high level to the experimental image. Under these imaging conditions the image contrast is quite robust with the change of the sample thickness. Figure 3(b) shows a thickness series of image calculated for a defocus of  $-50$  nm and a range of thickness of 2.4–8.4 nm by MACTEMPAS. It is hard to detect the contrast difference between these images. This is the reason why the experimental image shows a homogeneous contrast of the full particle,



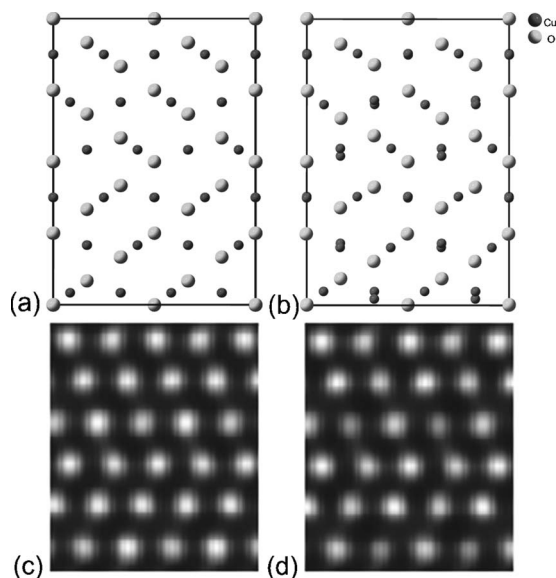


FIG. 4. 180° rotation twinning model (a) before relaxation and (b) after relaxation through first-principles calculation. [(c) and (d)] Simulated HRTEM images based on the model before and after relaxation, respectively.

although the inhomogeneity of thickness in the direction of projection is induced by the approximate sphericity of the particle.

The 180° rotation model is further refined by atomic relaxation based on first-principles calculation. Our first-principles calculations are performed using a plane-wave pseudopotential method. The exchange-correction energy is in the form of Perdew-Wang-91 with generalized gradient corrections. The cutoff energy is set to 396 eV in the present work. The Brillouin zones of the supercell are sampled with  $4 \times 3 \times 6$  Monkhorst meshes for the case of  $\text{Cu}_{48}\text{O}_{24}$ , and equivalent  $k$ -point sets are used for other cases. Atomic positions are fully relaxed. Before relaxation the energy for the 180° rotation model is  $-4.447$  eV per atom. The energy of the relaxed model is decreased to  $-4.490$  eV per atom. Comparison between the models before and after relaxation reveals only a very small displacement of some Cu atoms along the direction perpendicular to the twinning boundary. The maximum value of displacement is 0.03 nm as presented in Fig. 4(b). HRTEM simulations based on the models before and after relaxation show that almost no difference in contrast is induced by the small displacements as shown in Fig. 4(d). The simulated HRTEM image based on the relaxed model still fits well with the experimental image. Thus it can be concluded that the relaxed 180° rotation twinning model is reasonable in elucidating the experimental twinning images. Similar relaxation has been measured by phase-retrieval electron microscopy<sup>17</sup> and confirmed by first-principles calculation<sup>18</sup> in a  $\Sigma 3 \{111\}$  twinning boundary in  $\text{BaTiO}_3$ .

Other possible models are also investigated based on the operations stated above. All of them have fatal deficiencies. Mirror twinning model with the (111) O atom plane as the twin boundary leads to the simulated images with great deviation from the experimental image. Another mirror twinning model with the (111) Cu atom plane as twinning boundary results in too short interatomic distances across the boundary.

Besides the single twinning, we have also observed successive twinning stacking along the  $[111]$  axis and fivefold twinning phenomena. The formation of the successive twinning in these  $\text{Cu}_2\text{O}$  particles can be mainly attributed to lattice mismatch between  $\text{Cu}_2\text{O}$  and CNTs as substrate. At the interfaces where a high level stress accumulates, twins nucleate and grow through propagation of successive  $(1/6)\langle 112 \rangle$  dislocations. Besides that, it is reported that as the particles grow, the internal stresses become very important in the particles. In order to release the internal stress, one energetically favorable mechanism is the formation of twinning.<sup>19</sup> Moreover, fivefold twinning can be ascribed to an attempt to achieve highest symmetry of the surface structure, leading to the lowest surface energy during crystal growth. Although twinning affects the mechanical properties of nanoparticles in achieving more stable status, electrical properties of nanoparticles are not expected to be greatly affected, since there is no evident change of the structure and stoichiometry in the particles containing twinning.

In summary,  $\text{Cu}_2\text{O}$  growth twinning is clearly observed through HRTEM technique. The supercell twinning models are proposed. First-principles calculation as well as HRTEM simulation confirm the validity of the relaxed 180° rotation twin model. The mechanism of twinning and its effect on mechanical and electrical properties of  $\text{Cu}_2\text{O}$  nanoparticles are also discussed. The relaxed twinning model suggested in this letter can provide atomic basis for further study on twinning in  $\text{Cu}_2\text{O}$  or other materials that have similar structures as  $\text{Cu}_2\text{O}$ .

This research was financially supported by the Natural Science Foundation for the Outstanding Young Scientists of Hubei Province.

- <sup>1</sup>T. Mahalingam, J. S. P. Chitra, G. Ravi, J. P. Chu, and P. J. Sebastian, *Surf. Coat. Technol.* **168**, 111 (2003).
- <sup>2</sup>M. Yin, C. K. Wu, Y. B. Lou, C. Burda, J. T. Koberstein, Y. M. Zhu, and S. O'Brien, *J. Am. Chem. Soc.* **127**, 9506 (2005).
- <sup>3</sup>H. T. Zhang, D. M. Goodner, M. J. Bedzyk, T. J. Marks, and R. P. H. Chang, *Chem. Phys. Lett.* **395**, 296 (2004).
- <sup>4</sup>Y. Yu, L. L. Ma, W. Y. Huang, F. P. Du, J. C. Yu, J. G. Yu, J. B. Wang, and P. K. Wong, *Carbon* **43**, 651 (2005).
- <sup>5</sup>V. R. Palkar, P. Ayyub, S. Chattopadhyay, and M. Multani, *Phys. Rev. B* **53**, 2167 (1996).
- <sup>6</sup>B. K. Moss, P. Goodman, and A. W. S. Johnson, *J. Solid State Chem.* **73**, 268 (1988).
- <sup>7</sup>S. Asgari, *J. Mater. Process. Technol.* **155–156**, 1905 (2004).
- <sup>8</sup>I. Karaman, H. Sehitoglu, K. Gall, Y. I. Chumlyakov, and H. J. Maier, *Acta Mater.* **48**, 1345 (2000).
- <sup>9</sup>Y. M. Wang, A. M. Hodge, J. Biener, A. V. Hamza, D. E. Barnes, K. Liu, and T. G. Nieh, *Appl. Phys. Lett.* **86**, 101915 (2005).
- <sup>10</sup>Y. T. Zhu, X. Z. Liao, and R. Z. Valiev, *Appl. Phys. Lett.* **86**, 103112 (2005).
- <sup>11</sup>B. Sampedro, P. Crespo, A. Hernando, R. Litrán, J. C. Sánchez López, C. López Cartes, A. Fernandez, J. Ramírez, J. González Calbet, and M. Vallet, *Phys. Rev. Lett.* **91**, 237203 (2003).
- <sup>12</sup>C. J. Johnson, E. Dujardin, S. A. Davis, C. J. Murphy, and S. Mann, *J. Mater. Chem.* **12**, 1765 (2002).
- <sup>13</sup>M. Tanaka, M. Takeguchi, and K. Furuya, *Surf. Sci.* **433–435**, 491 (1999).
- <sup>14</sup>Andrew C. C. Yu, M. Mizuno, Y. Sasaki, H. Kondo, and K. Hiraga, *Appl. Phys. Lett.* **81**, 3768 (2002).
- <sup>15</sup>C. C. Yu, W. C. Cheng, D. C. Chen, Y. D. Yao, Y. Liou, and S. F. Lee, *J. Magn. Magn. Mater.* **239**, 323 (2002).
- <sup>16</sup>Y. Kaneno and T. Takasugi, *Mater. Sci. Eng., A* **393**, 71 (2005).
- <sup>17</sup>C. L. Jia and A. Thust, *Phys. Rev. Lett.* **82**, 5052 (1999).
- <sup>18</sup>W. T. Geng, Y. J. Zhao, A. J. Freeman, and B. Delley, *Phys. Rev. B* **63**, 060101 (2000).
- <sup>19</sup>M. José Yacamán, J. A. Ascencio, H. B. Liu, and J. G. Torresdey, *J. Vac. Sci. Technol. B* **19**, 1091 (2001).